

# Thermal Behavior and Kinetic Analysis of Enzymatic Hydrolysis Lignin and High-Density Polyethylene during Co-Pyrolysis

Weimin Chen, Xiaoyan Zhou,\* Shukai Shi, Thiphuong Nguyen, and Minzhi Chen

The thermal behaviors of enzymatic hydrolysis lignin (EHL), high-density polyethylene (HDPE), and their blend (50:50 wt.%) were revealed using thermogravimetric analysis coupled with Fourier transform infrared spectroscopy (TG-FTIR). A first-order reaction model (Coats-Redfern) and non-isothermal model-free method (Ozawa-Flynn-Wall) were applied to the TG experimental data to determine the pyrolysis kinetic parameters. The results showed that H<sub>2</sub>O and CO<sub>2</sub> were first released from the EHL due to the degradation of the weakly linked side chains. The degradation of lateral chains, the breakage of aromatic series in the EHL structure, and the  $\beta$  scission of HDPE led to the formation of H<sub>2</sub>O, CO<sub>2</sub>, C=O, aromatics, alkanes, and alkenes. Low intensities of H<sub>2</sub>O, CO<sub>2</sub>, alkanes, and alkenes were also observed in the final pyrolysis stage due to the degradation of lignin groups. Interactions during co-pyrolysis were observed in the pyrolysis stages of 390 to 542 °C and 563 to 790 °C. The activation energy values of EHL, HDPE, and their blend obtained by the Coats-Redfern method were 48.0 to 94.4 kJ/mol, 230.2 kJ/mol, and 42.7 to 260.1 kJ/mol, respectively. When the Ozawa-Flynn-Wall method was applied, activation energy ranges of 121.4 to 243.7 kJ/mol, 143.5 to 335.9 kJ/mol, and 74.8 to 260.9 kJ/mol for EHL, HDPE, and their blend, respectively, were observed.

*Keywords:* Co-pyrolysis; Lignin; High-density polyethylene; TG-FTIR; Kinetics

*Contact information:* College of Materials Science and Engineering, Nanjing Forestry University, Nanjing 210037, China; \*Corresponding author: zhouxiaoyan@njfu.edu.cn

## INTRODUCTION

Steam pretreatment and subsequent enzymatic hydrolysis has been applied to lignocellulosic materials for the production of bio-ethanol (Zhu and Pan 2010). Enzymatic hydrolysis lignin (EHL) is a promising residue of this process, and it has an annual worldwide yield of 200,000 tons (Zhou *et al.* 2013). The traditional utilization of EHL for energy recovery is focused on combustion due to its high heating value (Kumar *et al.* 2009). However, thermal conversion as a more effective recycling process could reduce the cost of bio-ethanol production and keep the process of steam pretreatment and enzymatic hydrolysis more competitive.

Pyrolysis is a simple process that can convert lignocellulosic materials into clean fuels and recover chemicals, especially bio-oil, bio-gas, and bio-char (Mohan *et al.* 2006; Yanik *et al.* 2007). However, biomass pyrolysis alone produces highly oxygenated compounds in its derived bio-oil, which results in many unstable properties, such as corrosion and high viscosity (Kanaujia *et al.* 2014). The co-pyrolysis of biomass with a synthetic polymer is an effective way to produce the bio-oil with lower water content and

less oxygenated compounds (Brebu and Spiridon 2012; Abnisa *et al.* 2013). The relative contents of the elements (C, H, and O) in the feedstock are re-adjusted, which strongly enhances the derived bio-oil. Moreover, the features of high carbon yield, low cost, and well-developed aromatic structure make EHL attractive as carbon precursor. The solid product (bio-char) derived from co-pyrolysis also demonstrates higher calorific values and greater porosity development in comparison to that derived from biomass alone (Chen *et al.* 2016).

However, the co-pyrolysis process comprises complex physical and chemical thermal behaviors, including various parallel and competing reactions (Çepelioğullar and Pütün 2013; Chin *et al.* 2014). The co-pyrolysis mechanism remains unknown. Kinetic analysis is essential to reveal the synergistic effect during co-pyrolysis and to better understand the thermal conversion mechanism. Moreover, the kinetic parameters can accurately predict the optimum conditions for the co-pyrolysis process to produce the desired products and design the thermochemical processes for fuel and chemical production (Mui *et al.* 2010; Rotliwala and Parikh 2011). Various methods have been applied to determine the kinetic parameters from the thermogravimetric (TG) data. Those methods are commonly classified into model-fitting and iso-conversional model-free methods (Miskolczi *et al.* 2004; Ebrahimi-Kahrizsangi and Abbasi 2008; Aboulkas *et al.* 2010). In particular, the model-free methods, such as the Ozawa-Flynn-Wall method, can determine the kinetic parameters of thermal decomposition and reveal the pyrolysis behaviors without any assumptions about the reaction order and specific fitting model (Luangkiattikhun *et al.* 2008; Ma *et al.* 2015).

In the present study, TG analysis coupled with Fourier transform infrared spectroscopy (TG-FTIR) was firstly applied in EHL from bio-ethanol production, high-density polyethylene (HDPE), and their blend (50:50 wt.%) to reveal their thermal behaviors. The released vapors were recorded in real-time by FTIR. Moreover, the kinetic parameters were determined based on the TG experimental data *via* the Coats-Redfern and Ozawa-Flynn-Wall methods. This information is essential for predicting the optimization of the co-pyrolysis process and controlling the thermal degradation process.

## EXPERIMENTAL

### Materials

EHL was derived from the corn stover residues of bio-ethanol production using alkaline solution extraction. The preparation and extraction for EHL and its FTIR spectrum were presented in our previous studies (Zhou *et al.* 2011; Chen *et al.* 2016). HDPE (model, 5000S; melt flow index, 0.95 g/10 min; density, 0.95 g/cm<sup>3</sup>; melting point, 130 °C) was purchased from Yangzi (Nanjing) Chemical Plastic Co., Ltd. (Nanjing, China). Both of the materials were first ground and sieved to a powder size of less than 0.154 mm using a mesh screen and dried at 60 °C in a vacuum oven. The blend of EHL and HDPE at a weight ratio of 50:50 was homogenized by rolling for 8 h.

### Methods

#### *Pyrolysis process*

The TG analysis (Netzsch STA449C, Bavaria, Germany) coupled with FTIR (Bruker FTIR Tensor 27 spectrometer, Berlin, Germany) was applied to the pyrolysis of

EHL, HDPE, and their blend. Samples with a mass of approximately 5 to 10 mg were heated up to 1000 °C at a heating rate of 20 °C/min. Each experiment was conducted with a 20 mL/min N<sub>2</sub> flow rate and a high purity of 99.99%. A flow cell and a pipe linking the TG analyzer and FTIR instrument were heated to 180 °C before each experiment started to prevent condensation of the released products. The products released from pyrolysis were recorded in real-time by applying the FTIR tracking mode with the wavenumber region of 400 to 4000 cm<sup>-1</sup>.

Nomenclature	
$K(T)$	Rate constant of the reaction
$A$	Pre-exponential factor (1/min)
$E_a$	Activation energy (kJ/mol)
$T$	Absolute temperature (K)
$T_i$	Initial pyrolysis temperature (K)
$T_f$	Final pyrolysis temperature (K)
$R$	Gas constant (J/mol K)
$\alpha$	Conversion rate (%)
$t$	Pyrolysis time (s)
$f(\alpha)$	Reaction model
$m_i$	The sample mass at initial pyrolysis temperature (g)
$m_\alpha$	The sample mass at the conversion rate of $\alpha$ (g)
$m_t$	The sample mass at time $t$ (g)
$m_f$	The sample mass at final pyrolysis temperature (g)
$\beta$	Heating rate (°C/min)
$g(\alpha)$	Integral form of conversion function
$p(x)$	Temperature integral

### Pyrolysis kinetics

The TG analyzer was applied to the pyrolysis of EHL, HDPE, and their blend using the three different heating rates of 20, 30, and 50 °C/min. Samples with a mass of approximately 5 to 10 mg were placed in an Al<sub>2</sub>O<sub>3</sub> crucible and heated to the final decomposition temperature of 1000 °C with a 20 mL/min N<sub>2</sub> flow rate. Each experiment was repeated three times, and only the average values were considered.

A first-order reaction model method (Coats-Redfern) and a non-isothermal model-free method (Ozawa-Flynn-Wall) were used to investigate the thermal behavior of EHL, HDPE, and their blend and determine the kinetic parameters. The pyrolysis of solid materials can be described using the equations shown below.



$$K(T) = Ae^{(-E_a/RT)} \quad (2)$$

$$\frac{d\alpha}{dt} = K(T)f(\alpha) \quad (3)$$

$$\alpha = (m_i - m_\alpha)/(m_i - m_f) \quad (4)$$

$$\beta = \frac{dT}{dt} = \frac{dT}{d\alpha} \frac{d\alpha}{dt} \quad (5)$$

Equation 6 was obtained and shown below by substituting Eq. 2 into Eq. 3, and subsequently combining Eqs. 3 and 5.

$$\frac{d\alpha}{dT} = \frac{A}{\beta} f(\alpha) e^{(-E_a/RT)} \quad (6)$$

$$g(\alpha) = \int_0^\alpha \frac{d\alpha}{f(\alpha)} \quad (7)$$

Equation 8 was derived by rearranging Eq. 6 and introducing Eq. 7.

$$g(\alpha) = \int_{T_i}^{T_f} \frac{1}{\beta} \cdot (A \cdot e^{-E_a/RT}) dT \quad (8)$$

Equations 9 and 10 were applied in the first-order reaction model.

$$f(\alpha) = 1 - \alpha \quad (9)$$

$$g(\alpha) = -\ln(1 - \alpha) \quad (10)$$

Hence, Eq. 8 was rewritten as presented in Eq. 11.

$$\ln(-\ln(1 - \alpha)/T^2) = (-E_a/R) \cdot (1/T) + \ln(ART^2/\beta E_a) \quad (11)$$

The experimental data derived from the TG analysis was applied in the Coats-Redfern method to determine the kinetic parameters. The  $E_a$  was estimated by the slope ( $-E_a/R$ ) of the fitted lines obtained from the plot of  $\ln(-\ln(1-\alpha)/T^2)$  vs.  $1000/T$ .

Moreover, Eq. 12 was derived as presented below by integrating and rearranging Eq. 6.

$$g(\alpha) = \int_0^\alpha \frac{d\alpha}{f(\alpha)} = \int_0^T \frac{A}{\beta} e^{-E_a/RT} dT = \frac{AE_a}{\beta R} \int_x^\infty u^{-2} e^{-u} du = \frac{AE_a}{\beta R} p(x) \quad (12)$$

$$x = E_a / RT \quad (13)$$

Doyle's approximation described as Eq. 14 was used in the Ozawa-Flynn-Wall method. Equation 15 was obtained as presented below by substituting  $p(x)$  into Eq. 12 and rearranging the equation.

$$\log[p(x)] = -2.315 + 0.457x \quad (14)$$

$$\log(\beta) = \log\left[\frac{AE_a}{Rg(\alpha)}\right] - 2.315 - 0.457 \frac{E_a}{RT} \quad (15)$$

The experimental TG data of this study were applied in the Ozawa-Flynn-Wall method to determine the pyrolysis kinetic parameters. The  $E_a$  was calculated from the slope ( $-0.457E_a/R$ ) of the fitted parallel lines obtained from the plot of  $\log(\beta)$  vs.  $1000/T$  with three different heating rates. The  $\alpha$  ranges of EHL, HDPE, and, co-pyrolysis were 10% to 50%, 10% to 90%, and 10% to 70%, which was based on the TG experimental data.

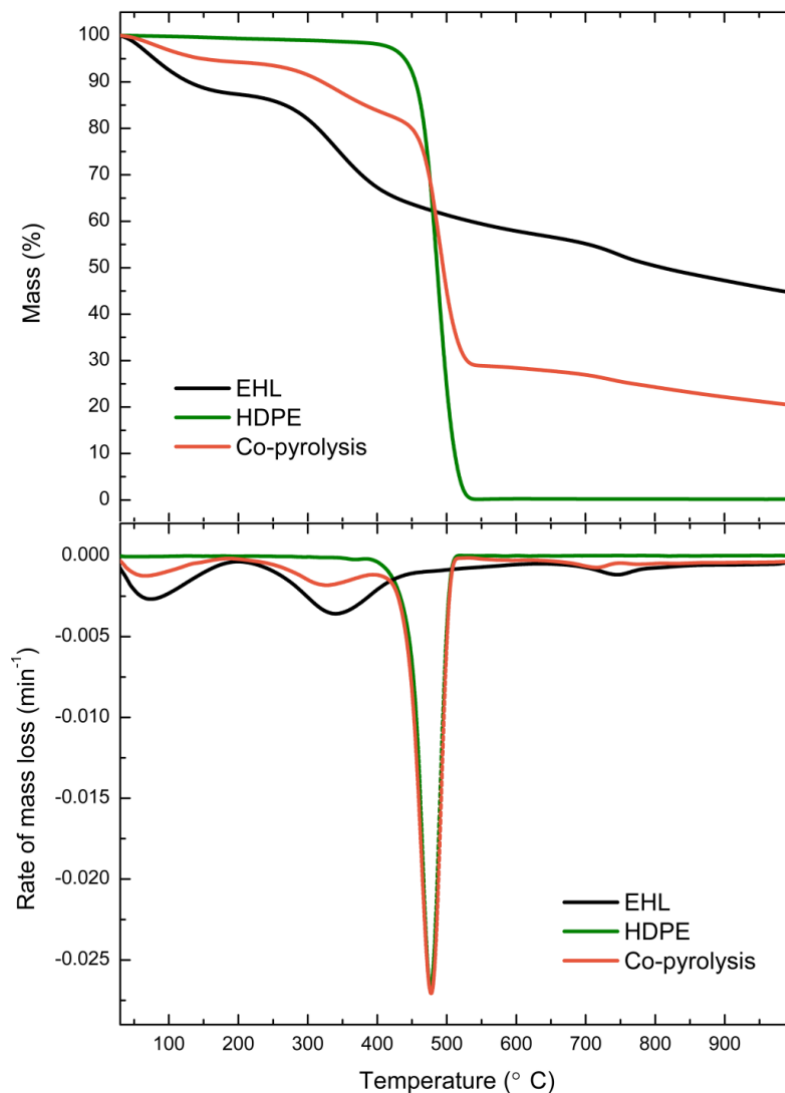


Fig. 1. TG and DTG curves of EHL, HDPE, and their blend with a heating rate of 20 °C/min

## RESULTS AND DISCUSSION

### TG Analysis

Figure 1 shows the TG and differential thermogravimetric (DTG) curves of EHL, HDPE, and their blend (weight ratio of 50:50) with the heating rate of 20 °C/min. EHL demonstrated three distinct weight loss stages, which indicated there was continuous decomposition during the entire pyrolysis process (25 °C to 1000 °C). The weight loss that occurred below 100 °C was related to moisture evaporation. A narrow thermal decomposition stage (397 °C to 520 °C) was observed for the HDPE, and no residue was retained, which implied there was total thermal conversion from the solid phase to the gas or liquid phase. Both the TG and DTG curves of the co-pyrolysis were between the two curves that corresponded to the individual pyrolysis of EHL and HDPE. The experimental value of the residue derived from co-pyrolysis ( $19.03 \pm 0.58\%$ ) at 1000 °C was lower than

the theoretical value ( $22.96 \pm 0.57\%$ ) calculated by the additivity rule that corresponded to the individual components. This fact implied the presence of interactions between those two materials.

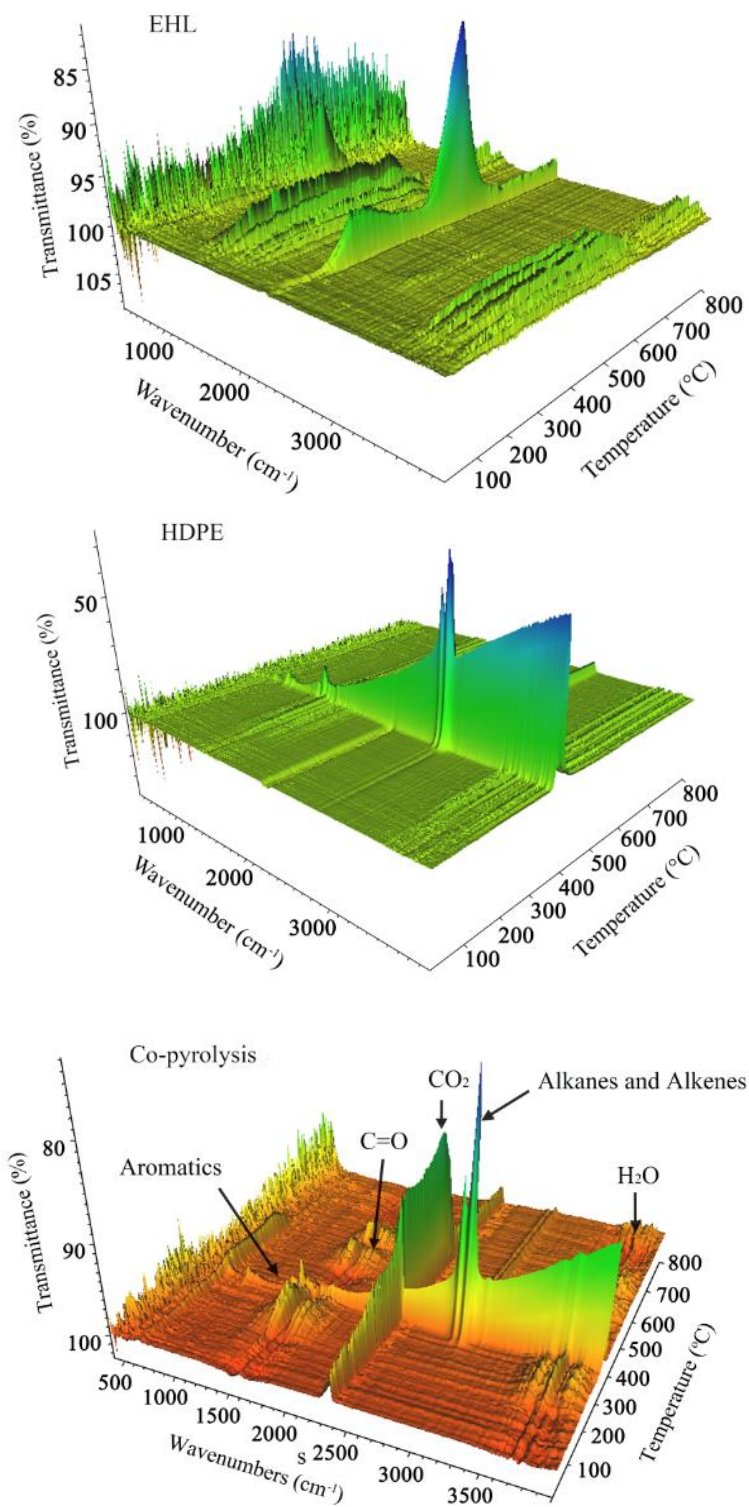


**Fig. 2.** 3D FTIR spectra of EHL, HDPE, and their blend

### Analysis of Three-Dimensional (3D) FTIR

The three-dimensional (3D) FTIR spectra of EHL, HDPE, and their blend are presented in Fig. 2. Several absorption peaks appeared in the 3D FTIR spectra, and their assignments to the specific releasing products are listed in Fig. 2 ( $\text{H}_2\text{O}$  at  $3725\text{ cm}^{-1}$ ; alkanes and alkenes at  $2912\text{ cm}^{-1}$ ;  $\text{CO}_2$  at  $2357\text{ cm}^{-1}$  and  $676\text{ cm}^{-1}$ ;  $\text{C}=\text{O}$  of aldehydes, ketones, and acids at  $1748\text{ cm}^{-1}$ ; aromatics at  $1514\text{ cm}^{-1}$ ) (Ren *et al.* 2013; Ma *et al.* 2015). The presence of  $\text{H}_2\text{O}$  and  $\text{CO}_2$  was observed in the first pyrolysis stage ( $40\text{ }^\circ\text{C}$  to  $190\text{ }^\circ\text{C}$ ) from Fig. 2 and the DTG curves in Fig. 1, which was attributed to the several decomposition reactions (*e.g.*, decarboxylation and dehydration). For instance, water released in this stage was generated from the cracking of aliphatic hydroxyls. The breakage of the lateral C-C bond in the EHL structure resulted in the production of carbon dioxide (Ren *et al.* 2013). This led to a mass loss of 7% in the first pyrolysis stage. The release of more products ( $\text{H}_2\text{O}$ ,  $\text{CO}_2$ ,  $\text{C}=\text{O}$ , aromatics, alkanes, and alkenes) was observed in the second pyrolysis stage ( $190\text{ }^\circ\text{C}$  to  $563\text{ }^\circ\text{C}$ ). Several decomposition reactions, *e.g.* dehydration, decarboxylation, demethoxylation, and demethylation, may have been responsible for the formation of the oxygenated products ( $\text{CO}_2$  and  $\text{C}=\text{O}$ ). Lateral chains with low thermal stability in the EHL structure may have generated  $\text{H}_2\text{O}$  and  $\text{CO}_2$  at this stage. The breaking of ether bonds, which were the bridges that linked the EHL units, may have also generated  $\text{CO}_2$  (Liu *et al.* 2008). The absorption intensity of  $\text{CO}_2$  derived from co-pyrolysis in the temperature region of HDPE decomposition was obviously higher than that released from EHL pyrolysis alone, which indicated the interaction between EHL and HDPE. The radicals from the HDPE decomposition were interacted with EHL, which results in the cracking reaction for oxygenated compounds (Marin *et al.* 2002). This may have been responsible for the lower mass of residue derived from co-pyrolysis as mentioned in the TG analysis. Aromatics ( $\text{C}_6$ ) were generated from the decomposition of aromatic series. Moreover, alkanes and alkenes were observed with strong intensities and reached their highest yields at this stage. Those products were primarily derived from the  $\beta$  scission of HDPE. Alkanes and alkenes derived from EHL with low intensities appeared in the third pyrolysis stage ( $563\text{ }^\circ\text{C}$  to  $790\text{ }^\circ\text{C}$ ) due to the degradation of lignin groups in the EHL.  $\text{H}_2\text{O}$  and  $\text{CO}_2$  were also observed at this stage. Some interactions between the radicals generated from HDPE decomposition and the EHL-derived char are responsible on the formation of  $\text{H}_2\text{O}$  and  $\text{CO}_2$ , which promotes further decomposition of EHL-derived char.

### Kinetic Analysis

Multiple heating rates (20, 30, and  $50\text{ }^\circ\text{C}/\text{min}$ ) were applied in the pyrolysis of EHL, HDPE, and their blend for the kinetic analysis. Figure 3 depicts the mass loss during the pyrolysis process of EHL, HDPE, and their blend expressed by temperature *versus*  $\alpha$ . All curves under the three heating rates exhibited the same decomposition trend. However, the curves shifted toward higher temperatures as the constant heating rate increased. This was related to the heat and mass transfer limitations in the materials, which resulted in the temperature difference between the crucible and materials (Vyazovkin *et al.* 2011). Moreover, the poor thermal conductivity of EHL and HDPE led to the temperature gradients among the materials. In other words, the mass transfer effect was caused by the fact that the interior temperature of the materials was generally higher than the external temperature, and in order to achieve the equivalent mass conversion of materials, higher temperatures and longer times were needed (Kumar *et al.* 2008; López-González *et al.* 2013).

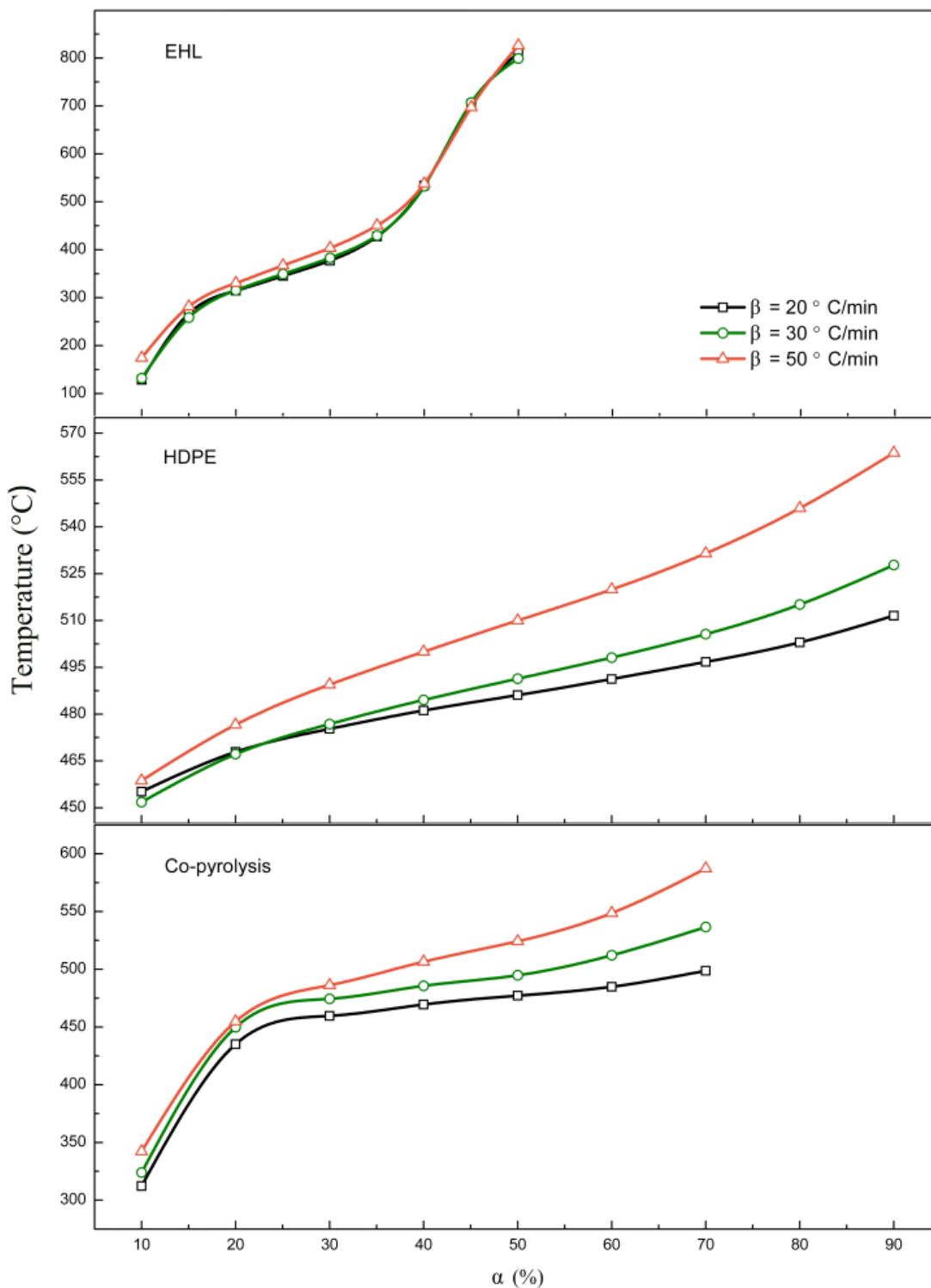


**Fig. 3.** Plots of temperature vs.  $\alpha$  for the pyrolysis process of EHL, HDPE, and their blend with the heating rates of 20, 30, and 50 °C/min

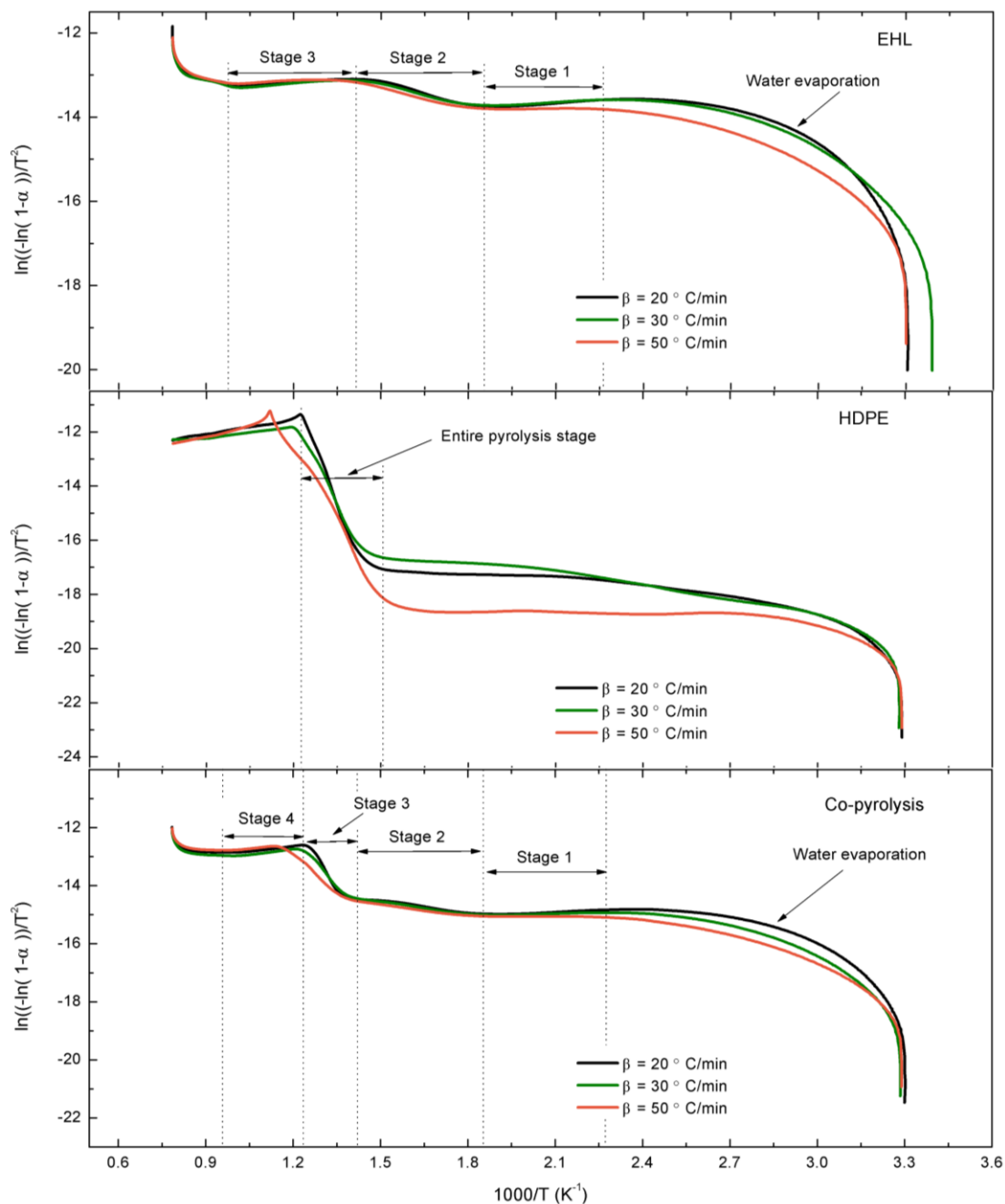


Fig. 4. Plots of  $\ln(-\ln(1-\alpha)/T^2)$  vs.  $1000/T$  for the pyrolysis process of EHL, HDPE, and their blend

Table 1. Kinetic Parameters for the Pyrolysis of EHL, HDPE, and their Blend using the Coats-Redfern Method

EHL			HDPE			Co-pyrolysis		
Temp. (°C)	$E_a$ (kJ/mol)	$R^2$	Temp. (°C)	$E_a$ (kJ/mol)	$R^2$	Temp. (°C)	$E_a$ (kJ/mol)	$R^2$
161-265	56.9±2.4	0.94	390-542	230.2	0.99	164-266	42.7±1.8	0.95
265-424	94.4±2.1	0.92				266-432	85.9±3.3	0.94
424-747	48.0±1.8	0.91				432-536	260.1±5.1	0.98
-	-	-				536-764	46.9±2.1	0.92

To examine the pyrolysis mechanism, the pyrolysis curves for EHL, HDPE, and their blend were plotted in the form  $\ln(-\ln(1-\alpha)/T^2)$  vs.  $1000/T$ , as presented in Fig. 4. EHL and HDPE exhibited totally different pyrolysis trends, and the co-pyrolysis showed the pyrolysis characteristics from both pure materials. The pyrolysis stages with different degradation mechanisms were determined by dividing the curve into several straight lines. The  $E_a$  values for the different pyrolysis stages were estimated from the slope of those straight lines, as presented in Table 1. All of the divided curves that corresponded to the pyrolysis stages were fitted to straight lines and had correlation coefficients higher than 0.90, which implied that the Coats-Redfern independent first-order reaction model fit the experimental data very well and that the kinetic parameters derived from this method were reliable. The estimated  $E_a$  values of EHL, HDPE, and their blend were in the range of 48.0 to 94.4 kJ/mol, 230.2 kJ/mol, and 42.7 to 260.1 kJ/mol, respectively. In particular, a lower  $E_a$  value (85.9 kJ/mol) for the co-pyrolysis in the pyrolysis temperature range of 266 to 432 °C was observed when compared to the EHL pyrolysis alone (94.4 kJ/mol). The interaction between the EHL and HDPE during the co-pyrolysis may have been responsible for the difference in the  $E_a$  values. The HDPE started to thermally decompose at higher temperatures and were completely thermally converted in the narrower temperature range (390 to 542 °C). This result was attributed to the lack of inherent water in its natural structure, which resulted in stronger chemical bonds. Therefore, HDPE had noticeably higher  $E_a$  values in comparison to EHL, which indicated that HDPE needed more energy to break its structure.

A model-free method (Ozawa-Flynn-Wall) was also used to determine the kinetic parameters. The pyrolysis experimental data derived from EHL, HDPE, and their blend with different heating rates was plotted in the form  $\log(\beta)$  vs.  $1000/T$ , and the results are presented in Fig. 5. The low correlation coefficients ( $R^2 = 0.87$  and  $0.67$ ) were observed for the fitted curves that corresponded to the section of water evaporation. All of the other fitted curves showed good coefficients of determination ( $R^2 > 0.90$ ), and were used to calculate the  $E_a$ . Figure 6 depicts the distribution of  $E_a$  expressed by  $E_a$  vs.  $\alpha$ . It should be noted that the  $E_a$  values vary with different heating rates, material, particle size, kinetic model, and instrument used for TG analysis (Vamvuka *et al.* 2003; Ma *et al.* 2015). Therefore, the  $E_a$  values based on the experimental data was valid for this study only.

Low  $E_a$  values were observed at the conversion rate of 10% for the pyrolysis of EHL and co-pyrolysis, which indicated that EHL underwent thermal decomposition rather easily. This fact was mainly attributed to the degradation of the side chains (methoxyl, carbonyl, hydroxy, and carboxy) weakly linked to the three basic units of EHL, *i.e.*, guaiacyl, syringyl, p-hydroxyl-phenyl, which was established by the FTIR analysis, as mentioned before (Liu *et al.* 2008). Moreover, the  $E_a$  values of EHL increased as  $\alpha$  increased, and the highest value was 243.7 kJ/mol. The three basic units in the EHL structure, which were heavily cross-linked with rather high thermal stability, needed a high  $E_a$  for decomposition (Biswas *et al.* 2016). In addition, a reaction favoring the formation of coke with low reaction activity also needed a high  $E_a$ . The  $E_a$  of co-pyrolysis first increased and then decreased as the conversion rate increased. This result was related to the presence of HDPE, which started to be degraded initially by random scission and resulted in the reduction of the polymerization degree and the length of polymeric linear chain. Thus, a high  $E_a$  was needed for the thermal degradation of the initial pyrolysis stage. Subsequently, the fragments with low molecular weight derived from random scission of HDPE started to decompose, which required lower  $E_a$  values (Miskolczi 2013).

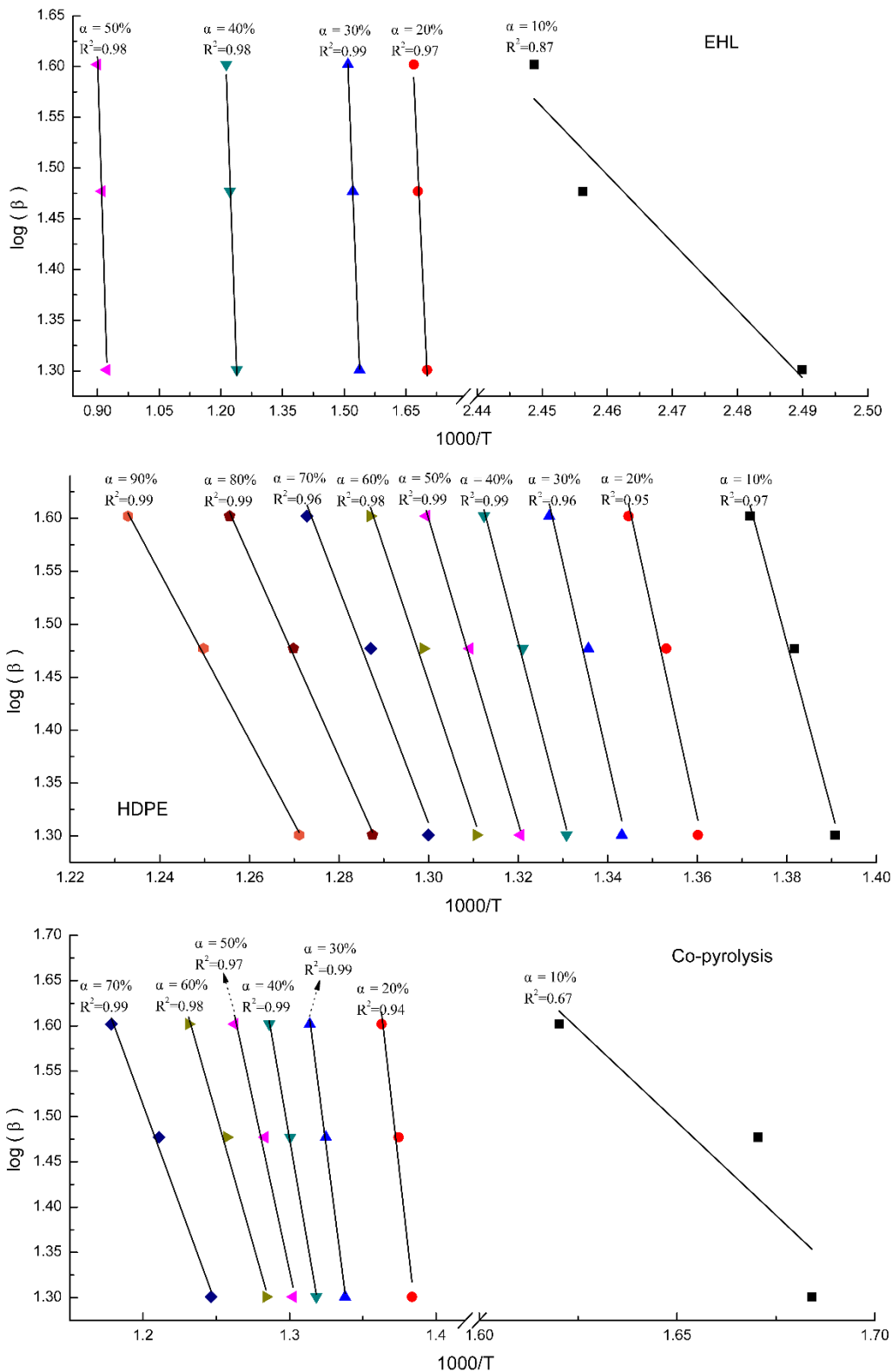


Fig. 5. Plots of  $\log(\beta)$  vs.  $1000/T$  for the pyrolysis process of EHL, HDPE, and their blend

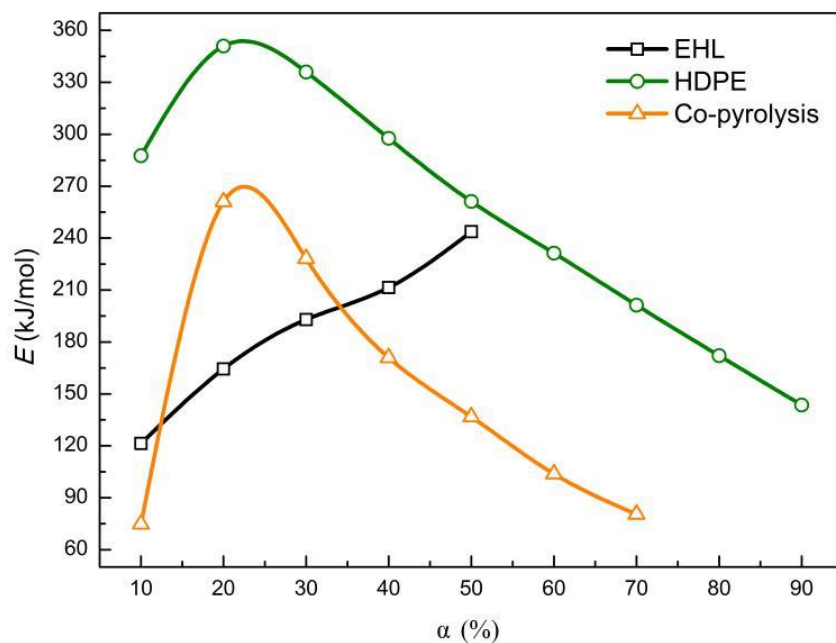


Fig. 6. The distribution of  $E_a$  expressed by  $E_a$  vs.  $\alpha$

## CONCLUSIONS

1. The side chains weakly linked to the three basic units of EHL were degraded in the first pyrolysis stage (40 to 190 °C), which resulted in the release of H<sub>2</sub>O and CO<sub>2</sub>. In the second pyrolysis stage (190 to 563 °C), the observed H<sub>2</sub>O, CO<sub>2</sub>, C=O, aromatics, alkanes, and alkenes were due to the degradation of lateral chains, the breakage of aromatic series in the EHL structure, and the  $\beta$  scission of HDPE. The degradation of lignin groups in the EHL structure led to the release of H<sub>2</sub>O, CO<sub>2</sub>, alkanes, and alkenes with low intensities in the final pyrolysis stage (563-790 °C).
2. Interactions during co-pyrolysis were observed in the pyrolysis stages of 390 to 542 °C and 563 to 790 °C. The radicals generated from HDPE decomposition were reacted with EHL, which results in the cracking reaction for oxygenated compounds and further decomposition of EHL-derived char. Those facts may increase the yield of liquid product (bio-oil) and lower the content of oxygenated compounds.
3. The  $E_a$  values of EHL, HDPE, and their blend obtained by the Coats-Redfern method varied in the range of 48.0 to 94.4 kJ/mol, 230.2 kJ/mol, and 42.7 to 260.1 kJ/mol, respectively. After the Ozawa-Flynn-Wall method was applied,  $E_a$  ranges of 121.4 to 243.7 kJ/mol, 143.5 to 335.9 kJ/mol, and 74.8 to 260.9 kJ/mol were observed for EHL, HDPE, and their blend, respectively.

## ACKNOWLEDGMENTS

The authors are grateful for the support from the projects of the National Natural Science Foundation of China (Grant No. 31270606 and Grant No. 31400515), the Natural Science Foundation of Jiangsu Province (Grant No. BK20161524), the Doctorate Fellows Foundation of Nanjing Forestry University, the Jiangsu Province Ordinary University Students' Scientific Research Innovation Project (Grant No. KYZZ16\_0320), and the Priority Academic Program Development of Jiangsu Higher Education Institutions (PAPD). This paper was sponsored by Qing Lan Project.

## REFERENCES CITED

- Abnisa, F., Daud, W. M. A. W., Ramalingam, S., Azemi, M. N. B., and Sahu, J. N. (2013). "Co-pyrolysis of palm shell and polystyrene waste mixtures to synthesis liquid fuel," *Fuel* 108, 311-318. DOI: 10.1016/j.fuel.2013.02.013
- Aboulkas, A., El Harfi, K., and El Bouadili, A. (2010). "Thermal degradation behaviors of polyethylene and polypropylene. Part I: Pyrolysis kinetics and mechanisms," *Energ. Convers. Manage.* 51(7), 1363-1369. DOI: 10.1016/j.enconman.2009.12.017
- Biswas, B., Singh, R., Kumar, J., Khan, A. A., Krishna, B. B., and Bhaskar, T. (2016). "Slow pyrolysis of prot, alkali and dealkaline lignins for production of chemicals," *Bioresource Technol.* 213, 319-326. DOI: 10.1016/j.biortech.2016.01.131
- Brebu, M., and Spiridon, I. (2012). "Co-pyrolysis of LignoBoost (R) lignin with synthetic polymers," *Polym. Degrad. Stabil.* 97(11), 2104-2109. DOI: 10.1016/j.polymdegradstab.2012.08.024
- Çepelioğullar, Ö., and Pütün, A. E. (2013). "Thermal and kinetic behaviors of biomass and plastic wastes in co-pyrolysis," *Energ. Convers. Manage.* 75, 263-270. DOI: 10.1016/j.enconman.2013.06.036
- Chen, W. M., Shi, S. K., Nguyen, T., Chen, M. Z., and Zhou, X. Y. (2016). "Effect of temperature on the evolution of physical structure and chemical properties of bio-char derived from co-pyrolysis of lignin with high-density polyethylene," *BioResources* 11(2), 3923-3936. DOI: 10.15376/biores.11.2.3923-3936
- Chin, B. L. F., Yusup, S., Al Shoaibi, A., Kannan, P., Srinivasakannan, C., and Sulaiman, S. A. (2014). "Kinetic studies of co-pyrolysis of rubber seed shell with high density polyethylene," *Energ. Convers. Manage.* 87, 746-753. DOI: 10.1016/j.enconman.2014.07.043
- Ebrahimi-Kahrizsangi, R., and Abbasi, M. H. (2008). "Evaluation of reliability of Coats-Redfern method for kinetic analysis of non-isothermal TGA," *T. Nonferr. Metal. Soc.* 18(1), 217-221. DOI: 10.1016/S1003-6326(08)60039-4
- Kanaujia, P. K., Sharma, Y. K., Garg, M. O., Tripathi, D., and Singh, R. (2014). "Review of analytical strategies in the production and upgrading of bio-oils derived from lignocellulosic biomass," *J. Anal. Appl. Pyrol.* 105, 55-74. DOI: 10.1016/j.jaap.2013.10.004
- Kumar, A., Wang, L., Dzenis, Y. A., Jones, D. D., and Hanna, M. A. (2008). "Thermogravimetric characterization of corn stover as gasification and pyrolysis feedstock," *Biomass Bioenerg.* 32(5), 460-467. DOI: 10.1016/j.biombioe.2007.11.004

- Kumar, M. N. S., Mohanty, A. K., Erickson, L., and Misra, M. (2009). "Lignin and its applications with polymers," *Journal of Biobased Materials and Bioenergy* 3(1), 1-24. DOI: 10.1166/jbmb.2009.1001
- Liu, Q., Wang, S., Zheng, Y., Luo, Z., and Cen, K. (2008). "Mechanism study of wood lignin pyrolysis by using TG-FTIR analysis," *J. Anal. Appl. Pyrol.* 82(1), 170-177. DOI: 10.1016/j.jaap.2008.03.007
- López-González, D., Fernandez-Lopez, M., Valverde, J. L., and Sanchez-Silva, L. (2013). "Thermogravimetric-mass spectrometric analysis on combustion of lignocellulosic biomass," *Bioresour Technol.* 143, 562-574. DOI: 10.1016/j.biortech.2013.06.052
- Luangkiattikhun, P., Tangsathikulchai, C., and Tangsathikulchai, M. (2008). "Non-isothermal thermogravimetric analysis of oil-palm solid wastes," *Bioresour Technol.* 99(5), 986-997. DOI: 10.1016/j.biortech.2007.03.001
- Ma, Z., Chen, D., Gu, J., Bao, B., and Zhang, Q. (2015). "Determination of pyrolysis characteristics and kinetics of palm kernel shell using TGA-FTIR and model-free integral methods," *Energ. Convers. Manage.* 89, 251-259. DOI: 10.1016/j.enconman.2014.09.074
- Marin, N., Collura, S., Sharypov, V. I., Beregovtsov, N. G., Baryshnikov, S. V., Kutnetzov, B. N., Cebolla, V., and Weber, J. V. (2002). "Copyrolysis of wood biomass and synthetic polymers mixtures. Part II: Characterisation of the liquid phases," *J. Anal. Appl. Pyrol.* 65(1), 41-55. DOI: 10.1016/S0165-2370(01)00179-6
- Miskolczi, N. (2013). "Co-pyrolysis of petroleum based waste HDPE, poly-lactic-acid biopolymer and organic waste," *J. Ind. Eng. Chem.* 19(5), 1549-1559. DOI: 10.1016/j.jiec.2013.01.022
- Miskolczi, N., Bartha, L., Deák, G. Y., Jóver, B., and Kalló, D. (2004). "Kinetic model of the chemical recycling of waste polyethylene into fuels," *Process Saf. Environ.* 82(3), 223-229. DOI: 10.1205/095758204323065984
- Mohan, D., Pittman, C. U., and Steele, P. H. (2006). "Pyrolysis of wood/biomass for bio-oil: A critical review," *Energ. Fuel.* 20(3), 848-889. DOI: 10.1021/ef0502397
- Mui, E. L. K., Cheung, W. H., Lee, V. K. C., and McKay, G. (2010). "Compensation effect during the pyrolysis of tyres and bamboo," *Waste Manage.* 30(5), 821-830. DOI: 10.1016/j.wasman.2010.01.014
- Ren, X. Y., Wang, W. L., Bai, T. T., Si, H., Chang, J. M., and Tian, H. X. (2013). "TG-FTIR study of the thermal-conversion properties of holo-cellulose derived from woody biomass," *Spectrosc. Spect. Anal.* 33(9), 2392-2397. DOI: 10.3964/j.issn.1000-0593(2013)09-2392-06
- Rotliwala, Y. C., and Parikh, P. A. (2011). "Thermal degradation of rice-bran with high density polyethylene: A kinetic study," *Korean J. Chem. Eng.* 28(3), 788-792. DOI: 10.1007/s11814-010-0414-1
- Vamvuka, D., Kakaras, E., Kastanaki, E., and Grammelis, P. (2003). "Pyrolysis characteristics and kinetics of biomass residuals mixtures with lignite," *Fuel* 82(15-17), 1949-1960. DOI: 10.1016/S0016-2361(03)00153-4
- Vyazovkin, S., Burnham, A. K., Criado, J. M., Pérez-Maqueda, L. A., Popescu, C., and Sbirrazzuoli, N. (2011). "ICTAC kinetics committee recommendations for performing kinetic computations on thermal analysis data," *Thermochim. Acta* 520(1-2), 1-19. DOI: 10.1016/j.tca.2011.03.034

- Yanik, J., Kornmayer, C., Saglam, M., and Yüksel, M. (2007). "Fast pyrolysis of agricultural wastes: Characterization of pyrolysis products," *Fuel Process. Technol.* 88(10), 942-947. DOI: 10.1016/j.fuproc.2007.05.002
- Zhou, X. Y., Zheng, F., Lv, C. L., Tang, L. J., Wei, K. C., Liu, X. Y., Du, G. B., Yong, Q., and Xue, G. (2013). "Properties of formaldehyde-free environmentally friendly lignocellulosic composites made from poplar fibres and oxygen-plasma-treated enzymatic hydrolysis lignin," *Compos. Part B-Eng.* 53, 369-375. DOI: 10.1016/j.compositesb.2013.05.037
- Zhou, X. Y., Tang, L. J., Zheng, F., Xue, G., Du, G. B., Zhang, W. D., Lv, C. L., Yong, Q., Zhang, R., Tang, B. J. (2011). "Oxygen plasma-treated enzymatic hydrolysis lignin as a natural binder for manufacturing biocomposites," *Holzforschung* 65, 829-833. DOI: 10.1515/HF.2011.093
- Zhu, J. Y., and Pan, X. J. (2010). "Woody biomass pretreatment for cellulosic ethanol production: Technology and energy consumption evaluation," *Bioresource Technol.* 101(13), 4992-5002. DOI: 10.1016/j.biortech.2009.11.007

Article submitted: October 9, 2016; Peer review completed: December 12, 2016; Revised version received and accepted: December 15, 2016; Published: December 19, 2016.  
DOI: 10.15376/biores.12.1.1150-1164